Residual Layer Thickness Control and Metrology in Jet and Flash Imprint Lithography

Shrawan Singhal[a], Ravikiran Attota[b], S.V. Sreenivasan[a1]
[a]Department of Mechanical Engineering, The University of Texas at Austin, 1 University Station C2200, Austin, TX 78712;
[b]Nanoscale Metrology Group, Semiconductor and Dimensional Metrology Division, National Institute of Standards and Technology, 100 Bureau Dr., Gaithersburg, MD 20899-8212

ABSTRACT

Jet-and-Flash Imprint Lithography (J-FIL) has demonstrated capability of high-resolution patterning at low costs. For accurate pattern transfer using J-FIL, it is necessary to have control of the residual layer thickness (RLT) of cured resist underneath features. Variation in RLT leads to critical dimension variation, thereby degrading device performance. Substrate nanotopography and feature density variation are two unavoidable sources of variation in RLT uniformity. The first part of this paper demonstrates the effect of these parameters on RLT variation. Through experiments and modeling, it has been observed that flatter wafers with lower nanotopography and thinner RLT lead to better RLT uniformity. However, for studying RLT variation, accurate metrology is critical. Currently, all metrology is done using destructive cross-section scanning electron microscopy (SEM), which may not be sufficient for process control. To this end, nondestructive optics-based methods, including the Through-focus Scanning Optical Microscopy (TSOM) method have been explored in this paper. Simulations reveal the potential to measure mean RLT, RLT variation, and uncertainty in feature dimension to an accuracy of 1 nm. Experimental validation and calibration are works in progress. Subsequent development of this technique can lead to a viable in-line metrology solution for RLT underneath features.

1. INTRODUCTION

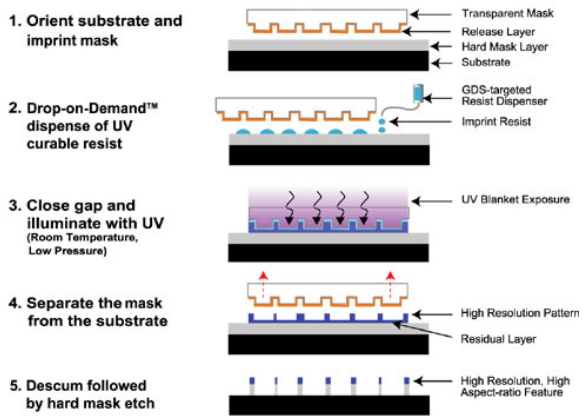

Imprint lithography (IL) has demonstrated sub-10 nm resolution at low cost. Jet and Flash Imprint Lithography or J-FIL is a variant of IL (also known as Step-and-Flash Imprint Lithography, S-FIL)[1-2]. It uses low pressure at room temperature and UV exposure to cure a low viscosity material that is dispensed using ink-jets as discrete drops of pico-liter volume. These drops fill in the mask features when the gap between the substrate and the mask is closed. After resist solidification, the mask is separated leaving the imprint material on the substrate. The low viscosity fluid leads to rapid fluid filling in the absence of a high compressive pressure, which results in lower machine complexity and high throughput. A process flow of the established technique has been illustrated in Figure 1.

Figure 1. Schematic of Jet and Flash Imprint Lithography (J-FIL)

Control over the resist residual layer thickness (RLT) underneath the patterned features is absolutely critical for the J-FIL process. It directly influences the transfer of the pattern into the substrate through subsequent processing steps such as descum etching. Any spatial variation in the RLT is reflected in the transferred pattern by way of variation in

[1] Email: sv.sreeni@mail.utexas.edu, Phone: 512-471-6546

Metrology, Inspection, and Process Control for Microlithography XXVI, edited by Alexander Starikov,
Proc. of SPIE Vol. 8324, 832434 · © 2012 SPIE · CCC code: 0277-786X/12/$18 · doi: 10.1117/12.916958

the critical dimension, which is detrimental to the performance of the manufactured device. Hence, understanding how RLT varies is extremely important for designing a process control framework. At the same time, it is also imperative to have robust non-destructive metrology for the RLT underneath features, which can complement process control for high throughput manufacturing.

One unavoidable source of variation in RLT is the non-planarity of the substrate. If the substrate-fluid-template sandwich is allowed to evolve or spread for a sufficiently long time prior to the UV exposure, the topography can lead to mm-scale variations in RLT. This variation can be qualitatively observed visually as changes in color. This observation has motivated a more detailed investigation into potential RLT non-uniformity and its mitigation, stemming from the coupling of substrate topography with the process time scale. Another source of RLT non-uniformity is variations in feature density across the patterned area. This variation is more subtle and requires the use of quantitative metrology, for which cross-section SEM has been the workhorse. Given the limitations of cross-section SEM in a high-throughput manufacturing environment, calibration and validation of a new optics-based method has been sought to bring out the within-wafer and across-wafer variations in RLT. However, prior to detailing the experiments and results, it is instructive to understand the nature of substrate topography and pattern density variations as applicable for this study. The influence of substrate topography on the J-FIL process has also been briefly stated with the help of a basic model of thin film flow between two elastic plates.

1.1 Substrate Topography

Deviations of any surface from ideal planarity is usually classified into three categories: (i) micro-roughness of spatial wavelength less than 0.1 mm and amplitude variation ≈10 nm, (ii) nanotopography [3] of spatial wavelength 0.1 mm to 20 mm and amplitude ≈100 nm to1um, and (iii) nominal shape of spatial wavelength greater than 20 mm. For semiconductor-process substrates, micro-roughness is usually minimal and well-mitigated by standard polishing processes like chemical mechanical polishing (CMP). Nominal shape, on the other hand, is well defined by the substrate geometry. However, nanotopography can remain a conspicuous artifact, even after multiple polishing steps. Current acceptable photolithography standards demand site flatness of less than 40 nm. This requires expensive polishing for substrates like Si. However, III-V substrates like GaAs wafers that are frequently used in the fabrication of optical devices like high-brightness LEDs are susceptible to the formation of columnar epitaxial defects. Moreover, because of their softer surface compared to Si, these substrates also cannot tolerate many polishing steps. Hence, they tend to exhibit significant nanotopography variation, beyond current acceptable photolithography standards of sub-40 nm site flatness, which makes using such processes extremely challenging. To this end, the influence of this topography variation on RLT has been studied using 50 mm diameter GaAs wafers. For comparison, 200 mm diameter Si wafers were also used as substrates for imprinting the same pattern. These wafers typically have much lower nanotopography compared to 50 mm GaAs as per vendor specifications.

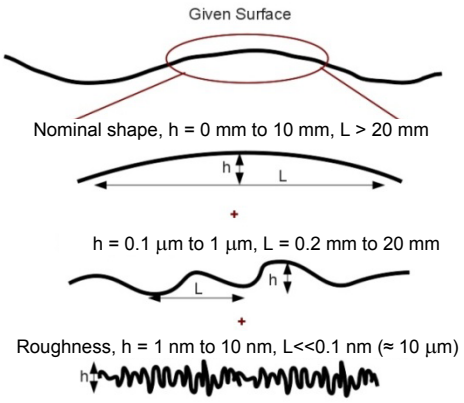

Figure 2. Illustration of topography of a surface depicting the classification of pre-patterning topographical features based on their spatial wavelength and amplitude.

The template for this pattern is a standard 65 mm x 65 mm fused silica template for step-and-repeat imprinting. It consists of several fields etched on a 13 mm x 13 mm mesa [4]. Each field is 1 mm x 0.5 mm in area and consists of 10 holes 80 nm deep. A large 0.15 mm x 0.2 mm rectangular feature is also present. This overall pattern is typically used for imprinting plasmonic devices like surface-emitting lasers. It must be noted that even the template is a polished surface and hence can exhibit similar nanotopography signatures as that of the substrate.

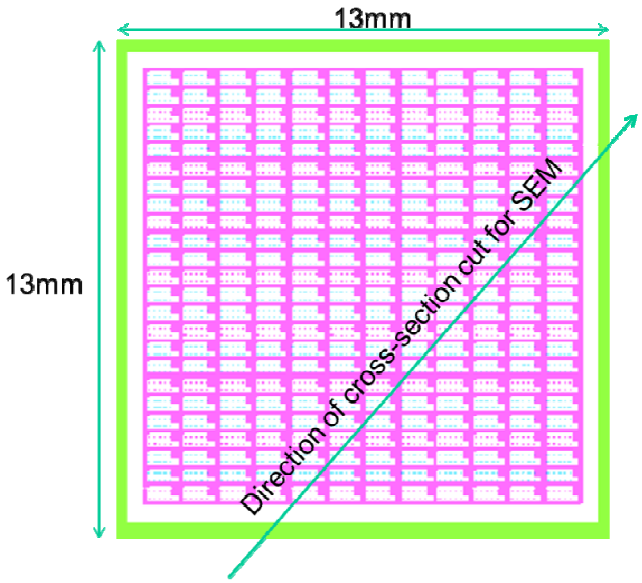

Figure 3. Layout of the active area of the template used. For a 50 mm substrate, the universal chuck would align the flat at an angle with a template. This results in a slanted cut for cross-sectional SEM.

1.2 Basic Modeling

The role of nanotopography in the process can be understood from a basic time evolution physical model. Fluid flow in domains that have much larger lateral length scales compared to height (thin films) can be solved using the lubrication approximation which assumes that the flow is predominantly parallel to the surface and the perpendicular pressure gradient is zero [5-7]. Neglecting gravity and using this approximation, fluid volume and momentum conservation along with thin plate bending for a thin fluid film sandwiched between two plates lead to the following governing equation:

$$12\mu\frac{\partial h}{\partial t} = D\vec{\nabla}.\left(h^3\vec{\nabla}\nabla^4\left(h + w_s - w_c\right)\right), \qquad (1)$$

where μ is the viscosity, $h(x,y,t)$ is the fluid film thickness, D is the bending rigidity of the template, $\vec{\nabla}$ is the spatial gradient vector, and $w_s(x,y)$ and $w_c(x,y)$ are time-invariant nominal topography of substrate and template, respectively. The substrate is rigidly held against a vacuum chuck without any bending deformation. The bending rigidity can be expressed as $D = \frac{Eb^3}{12(1-\nu^2)}$, where E, b, and ν are Young's modulus, thickness, and Poisson's ratio of the template, respectively. The materials used include fused silica for the template (E=73 GPa, ν =0.17) and Monomat$^{TM\#}$ (μ=10 cP) which is a proprietary UV-curable monomer from Molecular Imprints, Inc. From this equation it is revealed that a characteristic fluid distribution time-scale is inversely proportional to a characteristic fluid film thickness as —, where h_0 is a characteristic fluid film thickness that can be expressed as the mean RLT. If this time scale is high, as given by a low h_0, the final material distribution is primarily dictated by the initial dispensed fluid volume and pitch with minimal corruption due to the nanotopography of the substrate or template. If

however, the time scale is low, the fluid can re-distribute rapidly from its initial state, thereby leading to non-uniform RLT with a signature of the substrate or template nanotopography.

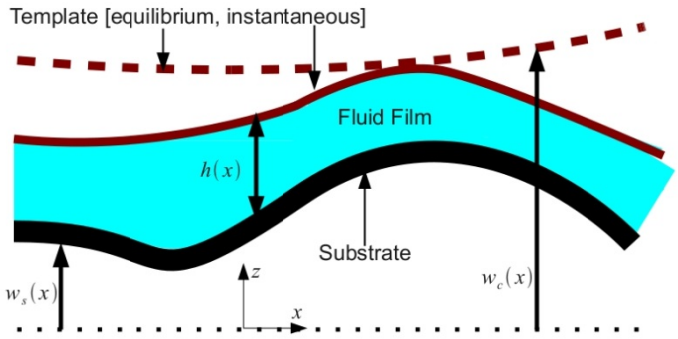

Figure 4. Geometry of the substrate-fluid-template sandwich as used in the basic model

1.3 Variation in Pattern Density

Pattern density variation typically manifests in the form of features of different CDs and/or pitch in a single imprinted field. At the transitions between these unequal sized features, the RLT may exhibit local non-uniformity at a similar spatial wavelength as that of the feature pitch. This non-uniformity also needs to be understood, which has been done using an exemplary full-wafer field with transition from an unpatterned to patterned region, as given in Figure 5. The template used has circular holes arranged in a locally hexagonal pattern of pitch ≈520 nm, nominal diameter of ≈235 nm, and depth of ≈110 nm. The patterned region on the template extends as an annular ring with an inner diameter of 8 mm and outer diameter of 49 mm. Hence, a transition exists between the patterned and unpatterned regions, as representative cases of varying feature density.

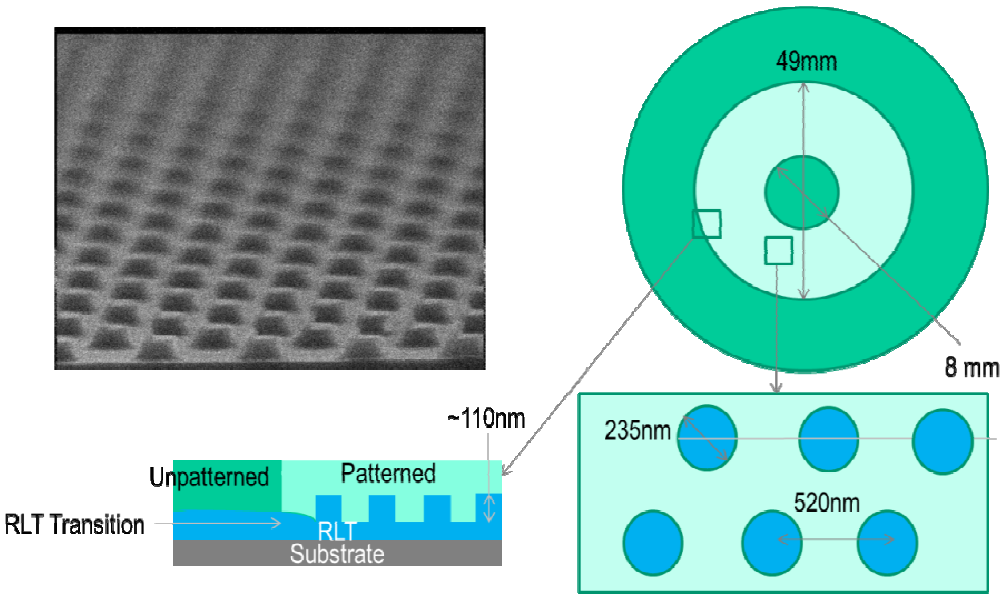

Figure 5. Illustration and SEM image of pattern used for establishing non-destructive metrology for studying pattern density variation.

2. STUDY OF RLT VARIATION

While minimizing RLT variation by keeping the characteristic process time scale high is necessary for efficient process control, it is also important to enable complete filling of the features by keeping the time scale sufficiently low. Due to this conflicting requirement, a combinatorial design of experiments has been undertaken to capture the influence of both substrate nanotopography and process spread time on RLT uniformity with the same pattern. The substrates used were 50 mm GaAs and 200 mm Si, as explained earlier. The mean RLT for both substrates was targeted to be either ≈50 nm or ≈15 nm. The spread time was also varied across a range of values. The tool used is an experimental test bed for step and repeat J-FIL. It is equipped with a universal chuck for handling wafers ranging from 50 mm to 200 mm in diameter.

2.1 Experimental Results

Experiments were conducted with a target RLT of 50 nm first. As seen in Figure 6, microscope images of the as-imprinted fields for this case indicate that there is significant RLT variation within the field. This can be estimated from the color transitions in the images. A uniform RLT of 50 nm should have transmitted a light brown color for the particular resist, but the images indicate color variations from blue to light brown, which approximately translates to a variation of ≈90 nm to ≈40 nm, respectively. Broadly, there seems to be no substantial difference in the pattern of the non-uniformity across the two types of substrates, thereby implying that the substrate nanotopography is not as dominant as the template nanotopography. However, the GaAs substrate does exhibit more local non-uniformity in the form of the lighter-colored circular regions. This may be attributed to the presence of epitaxial surface defects on the GaAs substrate. However, this conjecture cannot be confirmed, as it is infeasible to make the cut for the cross-section SEM through the local non-uniformity. Along with the substrate, the spread time does not seem to influence the RLT variation. Complete feature filling is confirmed by inspecting individual cells in the entire field for each spread time case. A representative image has been given in Figure 7. SEM metrology on a GaAs field has also been conducted. The results are shown in Figure 8 and confirm the variations seen qualitatively in Figure 6 with a range of 40.1 nm to 79.8 nm. For a feature depth of ≈100 nm, a 40 nm difference in RLT is not feasible from a subsequent etching perspective.

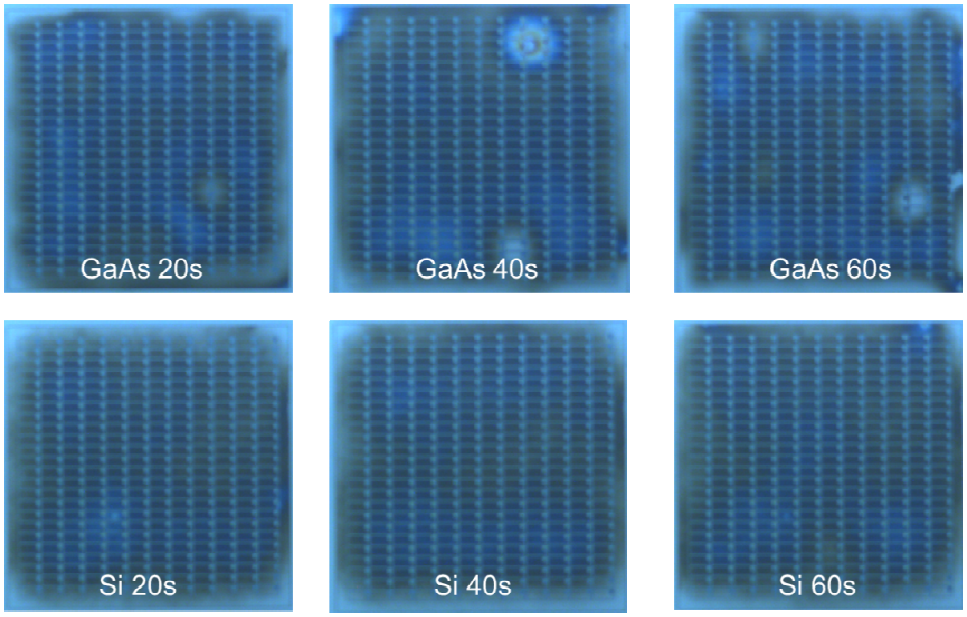

Figure 6. Images of imprinted fields for target thick RLT of ≈50 nm.

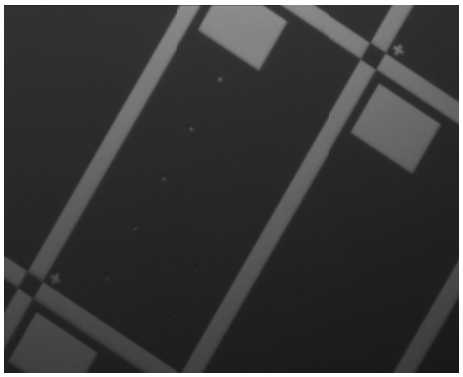

Figure 7. Optical microscopic inspection of individual cells reveals complete feature filling.

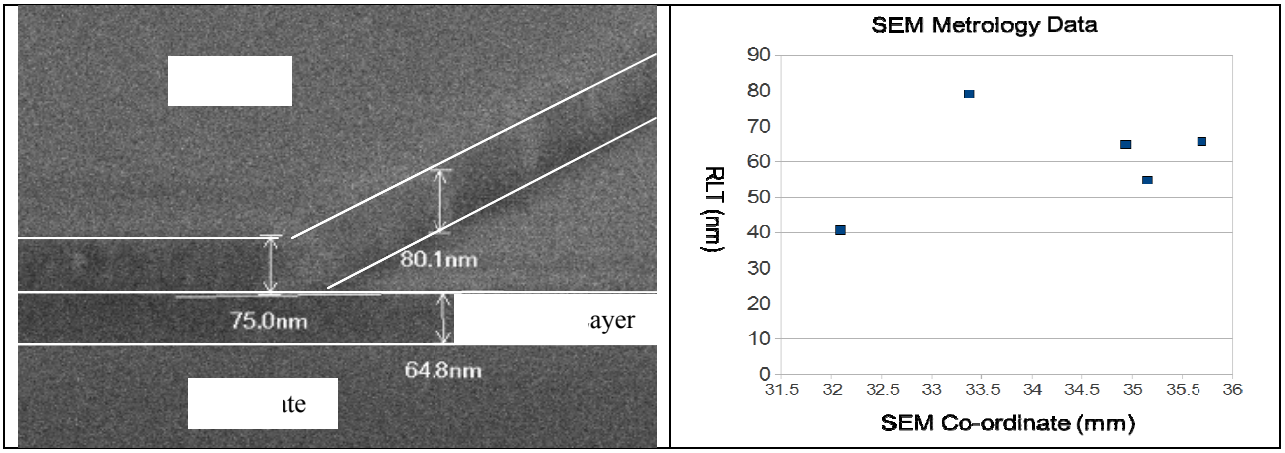

Figure 8. Results from SEM metrology. The left image shows an RLT of ≈65 nm and feature height of ≈80 nm at the 34.9 mm SEM co-ordinate from the right image.

However, the thin RLT case of ≈15 nm depicts a different picture. From qualitatively inspecting the uniform color seen in the images of the imprinted fields on both substrates, it was concluded that the RLT variation is significantly lower, compared to the thick RLT case. However, feature filling is satisfactory only at the highest spread time of 180 s, as seen in Figure 9. The substantially lower variation in RLT is also confirmed by measuring two GaAs samples with a cross-section SEM, as shown in Figure 10, which shows RLT range from 10.2 nm to 16.1 nm. Hence, while thin RLT is desirable from the perspective of low RLT variation and ease of subsequent descum etching, it can slow down throughput by taking longer to fill features. This has been overcome in J-FIL by going to lower volume drops. However, this was not possible on the experimental setup, making the compromise between pattern fidelity and feature filling necessary for the given tool configuration. Substrate nanotopography does not influence thin sub-20 nm RLT due to the long process time scale, thereby also confirming the model prediction.

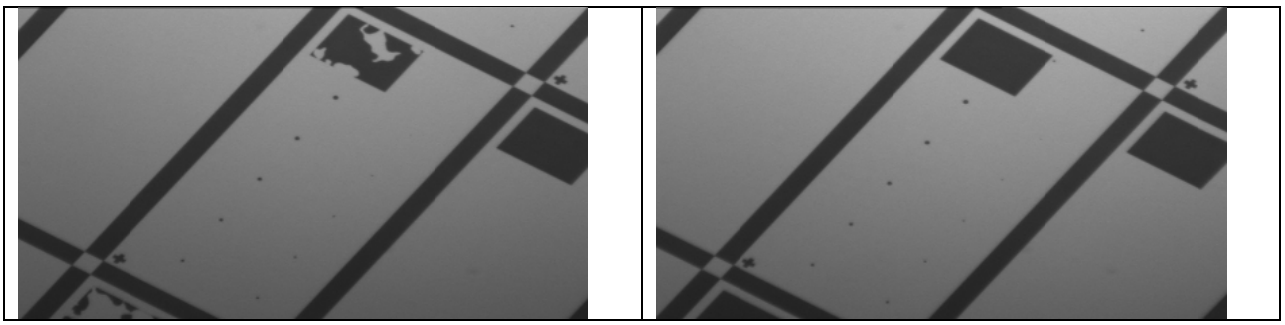

Figure 9. Optical microscopy images of individual fields showing incomplete filling with 60 s spread time (left) and complete filling with 180 s spread time (right). This trend is the same on both substrates.

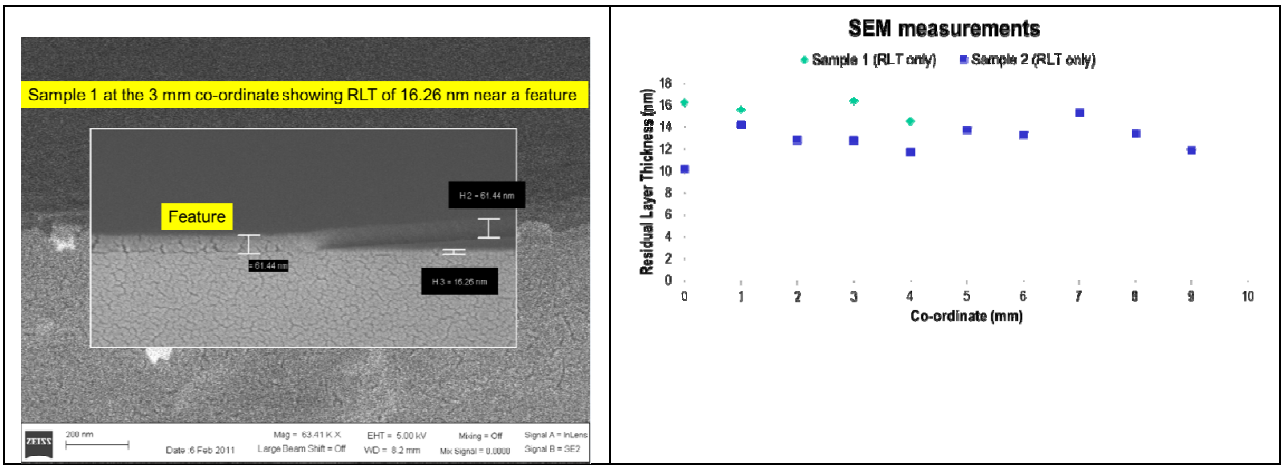

Figure 10. Cross-section SEM metrology for thin RLT shows lower variation than for thick RLT

3. DEVELOPMENT OF RLT METROLOGY

The influence of nanotopography on RLT non-uniformity was captured using a combination of visual, optical, and SEM inspection. However, quantifying the effect of pattern density perturbations requires accurate and repeatable metrology at the specific locations where feature density transitions take place. This is extremely cumbersome using current destructive techniques like cross-section SEM, which is usually acceptable for one-time process characterization at a few points, but not viable for wafer-wafer measurements at several locations in a high-throughput manufacturing environment. This has motivated the exploration of model-based non-destructive optical methods based on TSOM [8] for measuring the RLT under features.

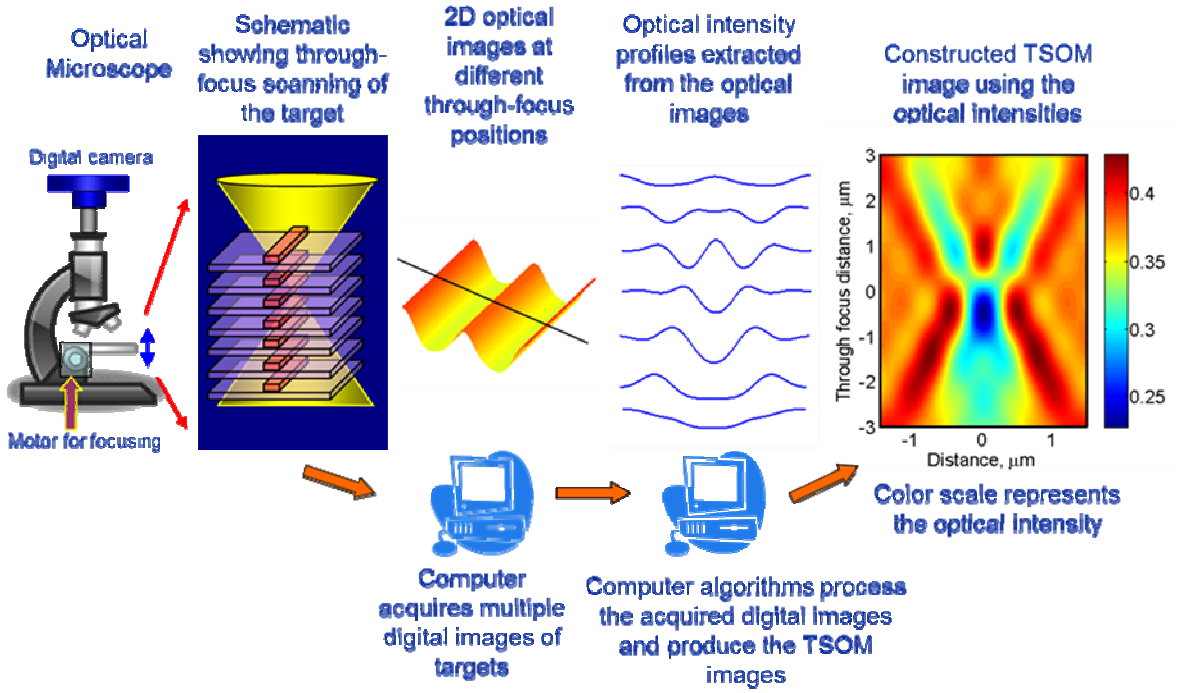

Figure 11. Method to construct TSOM images from a conventional optical microscope.

3.1 Metrology method (TSOM)

Instead of relying on a single best focus image, which is usually the norm in standard optical microscopy, TSOM relies on a number of through-focus images of the desired pattern, as given in Figure 11. The intensity profiles of these images give a unique signature that can be used to determine the nature of the pattern measured. With appropriate calibration, this method can be used to measure parameters in absolute values, such as the feature dimension. In addition, it can also be used for differential analyses; i.e., measuring the difference in one or more feature parameters. TSOM images of different samples can be compared for differential analysis as they give a unique signal which scales linearly with the magnitude of difference. This could be a useful technique for defect analysis also. So far, this technique has been validated for features on Si wafers, but has not been used for measuring RLT,; i.e., thickness of a polymeric film present underneath imprinted features, but above the Si substrate. This latter case is fundamentally different from the former case as the TSOM measurements for RLT require the optical signal to penetrate into the film beneath the features, which is not the same with features on Si wafers.. Calibration of this method is preceded by a full-fledged optical simulation with parameters across the full process window to understand the usefulness of the library approach method. Subsequent to this exercise, experimental validation can be conducted for absolute and differential TSOM. Modeling and simulation work are discussed in the next section. While experiments are underway, calibration and validation have not been completed yet.

3.2 Modeling and simulation

A spectrum of optical simulations of TSOM has been conducted for cases with varying mean RLT, as typically seen for J-FIL. This includes changes in feature dimensions for the template pattern shown in Figure 5 with pattern density variation. These simulations reveal usefulness of the differential TSOM method to identify changes in the RLT using intensity variations. This fact can be utilized to generate a calibration curve against which all RLT measurements may be compared to determine process performance. Moreover, the method is potentially useful for defect measurements, as it can also detect changes in feature dimensions, the signal for which can be decoupled from that of any difference in RLT. The parameter decoupling is one of the important characteristics of the TSOM method [8], and we expect similar behavior in the current application also. The optical simulation results with RLT parameters are shown in Figure 12.

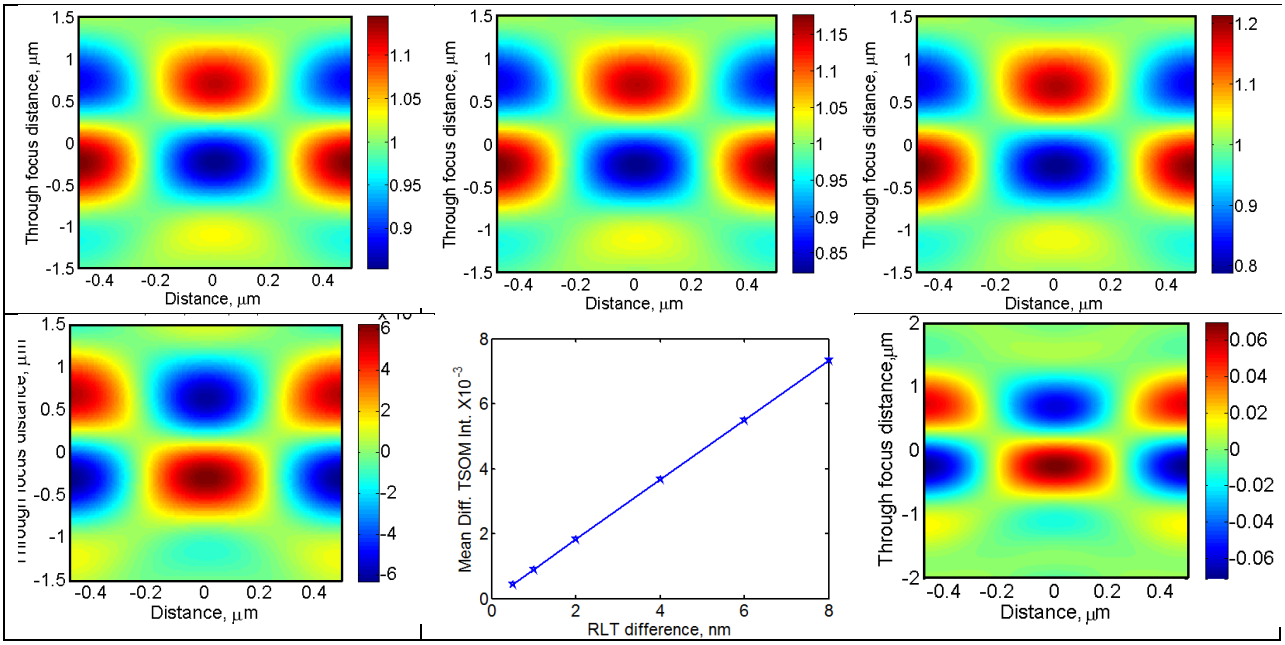

Figure 12. TSOM simulation results. (Top Left): RLT = 20 nm, (Top Middle): RLT = 30 nm, (Top Right): RLT = 40 nm, (Bottom Left): Differential TSOM image with 2 nm RLT difference, (Bottom Middle): Calibration curve for differential TSOM

image intensity against RLT difference showing linear trend, (Bottom Right): Differential TSOM image of 20 nm feature dimension difference decoupled from RLT difference.

4. CONCLUSIONS

Control over the RLT mean and variation is desirable for successful pattern transfer using J-FIL. Substrate and/or template nanotopography can cause undesired variation in the RLT, as predicted by a basic thin film fluid-structure model. This variation can be minimized by keeping the process time scale low by reducing the mean RLT. This has been demonstrated using a combinatorial set of experiments on two different substrates (50 mm GaAs and 200 mm Si) with two different target RLTs (15 nm and 50 nm).

Accurate metrology of RLT under features is imperative for control of RLT uniformity especially when feature density varies in the same imprinted field. Currently, this is done using destructive cross-section SEM, which is not a viable solution for generating spatial maps of RLT variation or for measuring wafer-wafer variation. To this end, a robust optics-based solution in the form of the TSOM method has been sought. Simulations indicate good potential accuracy of within 1 nm for measuring RLT mean, variation, and changes in feature dimension. Further calibration is underway to make the process more amenable for integration in the J-FIL process control framework.

ACKNOWLEDGEMENTS

This work was partially funded by DARPA Contract No. N66001-08-C-2040, the Texas Emerging Technology Funds program, and by a research grant from Molecular Imprints, Inc.

REFERENCES

[1] M. Colburn, A. Grot, M. Amistoso, B. J. Choi, T. Bailey, J. Ekerdt, S. V. Sreenivasan, J. Hollenhorst, and C. G. Willson, "Step and flash imprint lithography for sub-100-nm patterning," in *Proc. SPIE*, 2000, vol. 3997, p. 453.

[2] S. V. Sreenivasan, B. J. Choi, P. D. Schumaker, and F. Xu, "Status Of UV imprint lithography for nanoscale manufacturing," in *Comprehensive Nanoscience and Technology*, vol. 4, Oxford Academic Press, 2011, pp. 83-116.

[3] C.S. Xu, E. Zhao, R. Jairath, and W. Krusell, "Effects of silicon front surface topography on silicon oxide chemical mechanical planarization," *Electrochem. Solid-State Lett.*, vol. 1, no. 4, pp. 181-183, Oct. 1998.

[4] S.V. Sreenivasan et al., "Step and repeat imprint lithography processes," US Patent 7727453, Jun. 2010

[5] S. Reddy and R. Bonnecaze, "Simulation of fluid flow in the step and flash imprint lithography process," *MICROELECTRONIC ENGINEERING*, vol. 82, no. 1, pp. 60-70, Sep. 2005.

[6] S. Reddy, P. Schunk, and R. Bonnecaze, "Dynamics of low capillary number interfaces moving through sharp features," *PHYSICS OF FLUIDS*, vol. 17, no. 12, Dec. 2005.

[7] M. Colburn, B. Choi, S. Sreenivasan, R. Bonnecaze, and C. Willson, "Ramifications of lubrication theory on imprint lithography," *MICROELECTRONIC ENGINEERING*, vol. 75, no. 3, pp. 321-329, Sep. 2004.

[8] R. Attota, R.G. Dixson, J.A. Kramar, J.E. Potzick, A.E. Vladár, B. Bunday, E. Novak, and A. Rudack, "TSOM method for semiconductor metrology," Proc. of SPIE Vol. 7971, 79710T, 2011.

#Certain commercial equipment, instruments, or materials are identified in this document. Such identification does not imply recommendation or endorsement by NIST, nor does it imply that the products identified are necessarily the best available for the purpose.